

Geometric Approach to Digital Quantum Information

Chad Rigetti¹, Remy M ossen² and Michel Devoret¹

¹Department of Applied Physics, Yale University, New Haven, Connecticut 06520-8284, USA

²Groupe de Physique des Solides, Université Paris VI, campus Bouscaren, 140 rue de Lourmel, 75015 Paris, France

June 27, 2019

Abstract

We present geometric methods for uniformly discretizing the N -qubit Hilbert space, producing the equivalent of the Platonic solids in 2^N -dimensional Hilbert space. The group of transformations leaving these uniform Hilbertian polytopes invariant – known as the Clifford group – provides a general language for describing discrete transformations on N qubits. Our geometric approach to discretization sheds light on the relationships between the discrete quantum states and the generalized $=2$ rotations belonging to the Clifford group. We describe in detail the uniform Hilbertian polytope H_N for one and two qubits.

1 Introduction

The discrete nature of the configuration space for N classical bits is the key property allowing robustness of digital computation. The Hilbert space H_N for N qubits, on the other hand, is a 2^N -dimensional continuous complex manifold, and this poses challenging problems for quantum computation when the issues of gate fidelity and error correction are addressed. The continuity of the Hilbert space H_N can be described as follows: a general state can be written as

$$|i\rangle = \sum_{b_0 b_1 \dots b_{N-1}} t_{b_0 b_1 \dots b_{N-1}} |b_0 b_1 \dots b_{N-1} i\rangle$$

where $b_k \in \{0, 1\}$ is the value of the k -th qubit. The 2^N amplitudes $t_{b_0 b_1 \dots b_{N-1}}$ are complex numbers. Because of the normalization constraint and the arbitrariness of the overall phase of the wave function, an N qubit state can be parametrized by $2^{2N} - 2$ real numbers.

The continuous nature of H_N seems to be necessary for the exponential speedup of certain quantum information algorithms over classical ones. However, it is desirable, when dealing with the practicalities of implementing, optimizing, and testing a simple computing algorithm, to limit oneself to a finite subset $D_N \subset H_N$ of discrete states comprising a uniform sampling of the Hilbert space H_N . For instance, it is much easier to test for gate errors if all the target states belong to a finite set with well-defined properties. The nature and structure of the finite sets we have in mind is provided by the example of Platonic solids – geometrical figures such as the tetrahedron, cube and octahedron characterized by the geometric equivalence of their vertices – which represent discrete subsets uniformly spanning a sphere in R^3 . The requirement that D_N uniformly span H_N therefore suggests that we should seek the Hilbert space equivalent of the Platonic solids. That is, we wish to reduce H_N to a finite number of discrete states corresponding to the vertices of a uniform polytope in H_N . We call such subsets uniform Hilbertian polytopes (abbreviated H's) – the generalization of the Platonic solids to H_N .

Discrete sets of states have already been considered in quantum error-correcting codes, which work by selecting from a higher-dimensional Hilbert space (ie. coding space) a discrete set of states to be used in a computation. States in the coding space represent a basis in a lower dimensional computational space, while the higher dimensionality allows them to remain orthogonal over a class of transformations corresponding to computational errors. The stabilizer formalism can be used to characterize and produce quantum error-correcting codes, and also to analyze a broad class of quantum networks in the Heisenberg formalism [1]. However, the stabilizer formalism approaches the problem algebraically, and does not address the geometric relationship between the discrete quantum states, nor the relationships among the elements of the transformation group of the states (gates). The purpose of this paper is precisely to lay the ground work for a geometric approach to the problem of discretizing H_N ; ie. the problem of defining "digital" quantum information. In section 2 we treat this problem using results of stabilizer theory and the concept of generalized ± 2 rotations belonging to $SO(3)$, while in section 3 we use a purely geometric approach based on shelling the high dimensional lattices.

2 Discretization using the geometry of stabilizers

2.1 The 1-qubit case

Let us now make the discussion more concrete by examining the one-qubit Hilbert space, which can be mapped into a geometric 2-dimensional sphere embedded in R^3 , the Bloch sphere. A particularly interesting discrete subset of H_1 is the regular octahedron whose vertices correspond to the states at the

intersection of the Bloch sphere and the x ; y ; z axes.

$$\begin{aligned}
 j_z i &= j_0 i \\
 j_z i &= j_1 i \\
 j_x i &= \frac{j_0 i + j_1 i}{2} \\
 j_x i &= \frac{j_0 i - j_1 i}{2} \\
 j_y i &= \frac{j_0 i + i j_1 i}{2} \\
 j_y i &= \frac{j_0 i - i j_1 i}{2}
 \end{aligned}$$

These states and the octahedron they construct can be denoted H_1 , the UHP for the 1-qubit Hilbert space.

Starting from $j_z i = j_0 i$, all the elements of H_1 correspond to states directly accessible by standard NMR-type pulses performing $=2$ rotations. Therefore, even more important than the set of states itself is the subgroup of $SU(2)$ (the group of unitary complex 2×2 matrices with determinant 1) leaving H_1 invariant. This subgroup corresponds to the octahedral group O_h , of order 24, which is the group of rotations leaving the octahedron invariant (and by duality, the group leaving the cube invariant). We note that reflection operations, corresponding to exchange of the positive and negative axes of a single coordinate, while allowed in the context of group theory, are here excluded, since they do not correspond to physical operations.

Knowledge of how different elements of the octahedral group are related provides information on how to construct different one-qubit gates by forming 'words' from the group elements. For example, the Hadamard gate H is given by

$$H = \frac{1}{\sqrt{2}} \begin{pmatrix} 1 & 1 \\ 1 & 1 \end{pmatrix} = iR_x R_z R_x$$

where R_x and R_z are $=2$ rotations about the x - and z -axes, respectively. Similarly, knowledge of the structure of the groups leaving the higher-dimensional H 's invariant can be applied to the problem of quantum compilation. That is, it provides a means of decomposing a quantum gate into a product of rotations which can be implemented given the constraints on the Hamiltonian of the physical system.

In what follows, we describe a method that (1) identifies the physical quantum states corresponding to the vertices of H_N ; (2) describes the geometrical relationships among these states and (3) describes the structure of the group leaving the H 's invariant.

2.2 The uniform Hilbertian polytope H_N

As for the one-qubit case, the desired discrete set will be formed by eigenstates of the (generalized) Pauli matrices. However, for $N > 1$, the generalized Pauli matrices have degenerate eigenvalues, so additional prescriptions are required. The degeneracy can be lifted by choosing the states to be the common eigenvectors of the subsets of mutually commuting generalized Pauli matrices, which are called stabilizers.

Define the set S_N of generalized Pauli matrices on N qubits as the set of 4^N linearly independent $2^N \times 2^N$ matrices, which satisfy

$$\begin{aligned} \mathbf{Y}_j &= \mathbf{H}_j \text{ (Hermitian)} \\ \mathbf{Z}_j &= \mathbf{id} \text{ (Square root of unity)} \\ \text{Tr } \mathbf{Y}_j \mathbf{Y}_k &= 2^N \delta_{jk} \text{ (Orthogonal)} \end{aligned}$$

and are obtained by forming all unique tensor products of N standard 2×2 Pauli matrices. Any pair of generalized Pauli matrices either commute or anti-commute. Denote by S_N^a the subsets of mutually-commuting generalized Pauli matrices formed from the elements of S_N :

We seek to construct H_N ; the minimal uniform Hilbertian polytope for N qubits, such that:

1. It contains all the states $|b_0 b_1 \dots b_{N-1}\rangle$ corresponding to the classical bit configurations.
2. Each state of H_N is geometrically equivalent to all the others (uniformity)
3. The distance between two states $|j\rangle$ and $|k\rangle$, defined as:

$$d_{jk} = 2 \cos^{-1} (\langle \mathbf{H}_j | \mathbf{H}_k \rangle)$$

satisfies

$$d_{jk} = 2 \text{ for all } j, k$$

4. It is the largest set of states which satisfies the above requirements.

These desired properties are obtained if we adopt the following construction for the vertices of H_N

Definition 1 : Each vertex of H_N is a common eigenvector of a maximal subset $S_N^a \subset S_N$ of 2^N mutually-commuting generalized Pauli matrices on N qubits (stabilizer). That is, if \mathbf{H}_j is a generalized Pauli matrix on N qubits belonging

¹ Discretizations with a norm minimum distance may be useful and would be interesting to explore (for 2 qubits, see section 3). For one-qubit this could correspond, for instance, to the icosahedral geometry.

to the subset s_N^a ; $|j\rangle_i$ is an N -qubit state vector, and λ_j is an eigenvalue of σ_j belonging to the vector $|j\rangle_i$;

$$|j\rangle_i \in H_N, \quad \sigma_j |j\rangle_i = \lambda_j |j\rangle_i \text{ for all } |j\rangle_i \in s_N^a$$

As a consequence of this definition, and from the theory of stabilizers, we find:

a) For each s_N^a , which has 2^{N-1} elements different from the identity, we find 2^N different discrete states all separated by $\sigma_k = \pm 1$. Each state corresponds to a unique pattern of $\sigma_j = \pm 1$.

b) For each s_N^a and each of its nearest neighbours s_N^b (another stabilizer with whom it shares 2^{N-1} 0's), one can associate by a general algorithm a transformation from the common eigenvectors of s_N^a to those of s_N^b : That is, any two states of H_N are linked by a finite sequence of similarity transformations.

c) The similarity transformations are formed from generalized orthogonal =2 rotations of the form :

$$X_{kl}^a = \frac{1}{2} (|k\rangle\langle l| + |l\rangle\langle k|) \text{ where } [k; l] = 0 \text{ and } |k\rangle, |l\rangle \in s_N^a$$

The superscript a denotes a subset s_N^a to which both its 0's belong and the subscript specifies the 0's. The inverse operations are:

$$(X_{kl}^a)^{-1} = \frac{1}{2} (|k\rangle\langle l| - |l\rangle\langle k|) = -iX_{lk}^a$$

This definition implies that for any X

$$X^{\dagger}X = \text{id} \text{ (Unitary)}$$

$$X^4 = \text{id} \text{ (=2 Rotations)}$$

which is consistent with the property that a spin-1=2 acquires an overall phase of -1 when rotated by 2 :

d) The X 's generate the Clifford group C_N , defined as the normalizer of the Pauli group [2], which has the property of leaving H_N invariant (proof to follow).

e) The set S_N of generalized Pauli matrices on N qubits contains $s = \bigcup_{k=0}^{N-1} (2^{N-k} + 1)$ maximally-commuting subsets $s_N^a \subset S_N$. Each subset

²Strictly speaking a stabilizer is an Abelian subgroup of the Pauli group G_N , and is thus closed under multiplication. Since we are concerned primarily with the commutation properties of the Pauli matrices, we also refer to a maximal subset of mutually-commuting Pauli matrices as a stabilizer, whether or not it is a group. This choice emphasizes the close relationship between this work and the theory of stabilizers.

has 2^N elements, and contributes 2^N simultaneous eigenvectors. The uniform Hilbertian polytope on N qubits H_N therefore contains

$$V_N = 2^N \sum_{k=0}^{N-1} (2^N - k + 1)$$

vertices (states) [4]. Each s_N^a shares exactly half, or 2^{N-1} , of its elements with its nearest neighbour; 2^{N-2} with its second-nearest neighbour, etc., and each (non-identity) generalized Pauli matrix appears in $r = \frac{(2^N - 1)s}{4^N - 1} = \frac{V_N - s}{4^N - 1}$ independent sets. The following table gives the first values of V_N :

N	1	2	3	4	5
V_N	6	60	1080	36,720	2,423,520

It is easy to show that V_N grows as $2^{\frac{N^2+3N}{2}}$. The information content of H_N is therefore super-extensive in N . It is a remarkable property, even if it is insufficient for algorithms which would be exponentially faster than classical ones.

2.3 The 1-qubit case, revisited

The standard 2×2 Pauli matrices are:

$$\begin{array}{ll} w = 0 = \begin{pmatrix} 1 & 0 \\ 0 & 1 \end{pmatrix} & x = 2 = \begin{pmatrix} 0 & 1 \\ 1 & 0 \end{pmatrix} \\ y = 3 = \begin{pmatrix} 0 & i \\ i & 0 \end{pmatrix} & z = 1 = \begin{pmatrix} 1 & 0 \\ 0 & 1 \end{pmatrix} \end{array}$$

The present numbering scheme for the Pauli matrices is chosen to conform to Gotteman's ingenious binary digit notation [2]).

These matrices multiply as follows:

$$\begin{array}{ll} x \cdot y = y \cdot x = i \cdot z \\ y \cdot z = z \cdot y = i \cdot x \\ z \cdot x = x \cdot z = i \cdot y \\ \frac{2}{x} = \frac{2}{y} = \frac{2}{z} = w \end{array}$$

There are 3 sets of mutually commuting matrices: $s_1^1 = f_w; xg; s_1^2 = f_w; yg$ and $s_1^3 = f_w; zg$: The first 2 states of H_1

$$\begin{array}{l} j^z i = j^0 i \\ j^z i = j^1 i \end{array}$$

are the eigenvectors of j^z and $j^z = 1$ (computational basis). The second pair,

$$j^x i = \frac{j^0 i + j^1 i}{2}$$

$$j^x i = \frac{j^0 i - j^1 i}{2}$$

are the eigenvectors of $\mathbf{0}$ and $\mathbf{x} = \mathbf{z}$. The third pair

$$\begin{aligned} \mathbf{y}_i &= \frac{\mathbf{p}_i + \mathbf{i}_j \mathbf{i}_j}{\sqrt{2}} \\ \mathbf{z}_i &= \frac{\mathbf{p}_i - \mathbf{i}_j \mathbf{i}_j}{\sqrt{2}} \end{aligned}$$

correspond to $\mathbf{0}$ and $\mathbf{y} = \mathbf{z}$:

There are 3 orthogonal $=2$ rotations, which form the 'seed' of H_1 :

$$X_{01}^1 = \frac{1}{\sqrt{2}} (\mathbf{0} + \mathbf{i}_1)$$

$$X_{02}^2 = \frac{1}{\sqrt{2}} (\mathbf{0} + \mathbf{i}_2)$$

$$X_{03}^3 = \frac{1}{\sqrt{2}} (\mathbf{0} + \mathbf{i}_3)$$

The diagonalization of the seed elements leads to 6 eigenstates – the states appearing on the Bloch sphere.

Each of these rotations has an inverse:

$$(X_{0k}^k)^{-1} = iX_{k0}^k = \frac{1}{\sqrt{2}} (\mathbf{0} - \mathbf{i}_k)$$

It is easy to verify that

$$(X_{0k}^k)^2 = \frac{1}{2} (\mathbf{0} + \mathbf{i}_k)^2 = \mathbf{i}_k$$

and that the X^0 's are mapped into one another by similarity transformation:

$$\begin{aligned} X_{0j}^j X_{0i}^i X_{0j}^j &= \frac{1}{2} \frac{1}{\sqrt{2}} (\mathbf{0} + \mathbf{i}_j) (\mathbf{0} + \mathbf{i}_i) (\mathbf{0} - \mathbf{i}_j) \\ &= \frac{1}{2} \frac{1}{\sqrt{2}} (2\mathbf{0} + 2i_{ijk} \mathbf{i}_k) \\ &= X_{0k}^k \quad \text{if } i_{ijk} = 1 \\ &= -X_{0k}^k \quad \text{if } i_{ijk} = -1 \end{aligned}$$

This implies that each X^0 transforms a member of H_1 into its neighbour.

Proof. If

$$X_{0j}^j X_{0i}^i = X_{0i}^i X_{0j}^j$$

and if

$$i_{(j)} = X_{0j}^i$$

then

$$\begin{aligned}
 X^i X^j (X^i)^{-1} &= X^i X^j j_{ji} \\
 &= j X^i j_{ji} \\
 &= j_{ji}
 \end{aligned}$$

therefore j_{ji} is an eigenvector of X^k . ■

The X^i 's with their inverse generate a 24 element group isomorphic to the octahedral group of pure rotations which leaves the octahedron or the cube invariant. We would now like to show how these notions can easily be generalized to the two-qubit Hilbert space.

2.4 The 2-qubit uniform Hilbertian polytope H_2

The set of generalized Pauli matrices for 2 qubits S_2 comprises $4^2 = 16, 2^2 = 2^2$ matrices given by $=$ ³:

³We write the index on the 0's in binary, then concatenate the two strings to form the new index for the 0's: For example, $y = 3 = 11_2$, $z = 1 = 01_2 = 1101_2 = 13$

The relationship between multiplication of generalized Pauli matrices and operations on binary strings is well-known [5].

$$\begin{array}{ll}
w_w = 0 = \begin{smallmatrix} 2 & 1 & 0 & 0 & 0 & 3 \\ 6 & 0 & 1 & 0 & 0 & 7 \\ 4 & 0 & 0 & 1 & 0 & 5 \end{smallmatrix} & w_z = 1 = \begin{smallmatrix} 2 & 1 & 0 & 0 & 0 & 3 \\ 6 & 0 & 1 & 0 & 0 & 7 \\ 4 & 0 & 0 & 1 & 0 & 5 \end{smallmatrix} \\
w_x = 2 = \begin{smallmatrix} 2 & 0 & 0 & 0 & 1 & 3 \\ 0 & 1 & 0 & 0 & 0 & 0 \\ 4 & 1 & 0 & 0 & 0 & 7 \\ 4 & 0 & 0 & 0 & 1 & 5 \end{smallmatrix} & w_y = 3 = \begin{smallmatrix} 2 & 0 & 0 & 0 & 1 & 3 \\ 0 & i & 0 & 0 & 0 & 0 \\ 6 & i & 0 & 0 & 0 & 7 \\ 4 & 0 & 0 & 0 & i & 5 \end{smallmatrix} \\
z_w = 4 = \begin{smallmatrix} 2 & 0 & 0 & 1 & 0 & 3 \\ 1 & 0 & 0 & 0 & 0 & 0 \\ 4 & 0 & 1 & 0 & 0 & 7 \\ 4 & 0 & 0 & 1 & 0 & 5 \end{smallmatrix} & z_z = 5 = \begin{smallmatrix} 2 & 0 & 0 & i & 0 & 3 \\ 1 & 0 & 0 & 0 & 0 & 0 \\ 6 & 0 & 1 & 0 & 0 & 7 \\ 4 & 0 & 0 & 1 & 0 & 5 \end{smallmatrix} \\
z_x = 6 = \begin{smallmatrix} 2 & 0 & 0 & 0 & 1 & 3 \\ 0 & 1 & 0 & 0 & 0 & 0 \\ 4 & 6 & 1 & 0 & 0 & 7 \\ 4 & 0 & 0 & 0 & 1 & 5 \end{smallmatrix} & z_y = 7 = \begin{smallmatrix} 2 & 0 & 0 & 0 & 1 & 3 \\ 0 & i & 0 & 0 & 0 & 0 \\ 6 & i & 0 & 0 & 0 & 7 \\ 4 & 0 & 0 & 0 & i & 5 \end{smallmatrix} \\
x_w = 8 = \begin{smallmatrix} 2 & 0 & 0 & 1 & 0 & 3 \\ 0 & 0 & 1 & 0 & 0 & 0 \\ 4 & 6 & 0 & 0 & 0 & 7 \\ 4 & 1 & 0 & 0 & 0 & 5 \end{smallmatrix} & x_z = 9 = \begin{smallmatrix} 2 & 0 & 0 & i & 0 & 3 \\ 0 & 0 & 1 & 0 & 0 & 0 \\ 6 & 0 & 0 & 0 & 1 & 7 \\ 4 & 1 & 0 & 0 & 0 & 5 \end{smallmatrix} \\
x_x = 10 = \begin{smallmatrix} 2 & 0 & 1 & 0 & 0 & 3 \\ 0 & 0 & 0 & 1 & 0 & 0 \\ 4 & 6 & 0 & 0 & 1 & 0 \\ 4 & 0 & 1 & 0 & 0 & 5 \end{smallmatrix} & x_y = 11 = \begin{smallmatrix} 2 & 0 & 1 & 0 & 0 & 3 \\ 0 & 0 & 0 & i & 0 & 0 \\ 6 & 0 & 0 & i & 0 & 7 \\ 4 & 0 & i & 0 & 0 & 5 \end{smallmatrix} \\
y_w = 12 = \begin{smallmatrix} 2 & 1 & 0 & 0 & 0 & 3 \\ 0 & 0 & i & 0 & 0 & 0 \\ 4 & 6 & 0 & 0 & i & 7 \\ 4 & i & 0 & 0 & 0 & 5 \end{smallmatrix} & y_z = 13 = \begin{smallmatrix} 2 & i & 0 & 0 & 0 & 3 \\ 0 & 0 & 0 & i & 0 & 0 \\ 6 & 0 & 0 & 0 & i & 7 \\ 4 & i & 0 & 0 & 0 & 5 \end{smallmatrix} \\
y_x = 14 = \begin{smallmatrix} 2 & 0 & i & 0 & 0 & 3 \\ 0 & 0 & 0 & i & 0 & 0 \\ 4 & 6 & 0 & 0 & i & 7 \\ 4 & 0 & i & 0 & 0 & 5 \end{smallmatrix} & y_y = 15 = \begin{smallmatrix} 2 & 0 & i & 0 & 0 & 3 \\ 0 & 0 & 0 & 0 & 0 & 1 \\ 6 & 0 & 0 & 1 & 0 & 7 \\ 4 & 0 & 1 & 0 & 0 & 5 \\ i & 0 & 0 & 0 & 0 & 0 \end{smallmatrix} \\
& \qquad \qquad \qquad 1 & 0 & 0 & 0 & 0
\end{array}$$

The products of these matrices can easily be found from

$$= (\quad) (\quad) = (\quad) (\quad)$$

It is obvious from this relation and the multiplication table of 2 2 Pauli matrices that if we enlarge the set to include elements of the form ; i and i, we form a group, the Pauli group.

The subsets of mutually-commuting elements of S_2 forming Abelian subsets are⁴

⁴Constructing the subsets of mutually commuting Pauli matrices can be done through a series of logical steps. The key is to note that $[j_k; l_m] = 0$ requires either

$$[j_1; l_1] = [k_1; m_1] = 0$$

or

$$f_{j_1; l_1} g = f_{k_1; m_1} g = 0$$

subset #	letter notation	number notation	$g = \frac{Q}{j}$
1	$f_{wwi} wzi zwj zzg$	$f_{0i} 1i 4i 5g$	1
2	$f_{wwi} wxi zwj zxg$	$f_{0i} 2i 4i 6g$	1
3	$f_{wwi} wyi zwj zyg$	$f_{0i} 3i 4i 7g$	1
4	$f_{wwi} wzj xwi xzg$	$f_{0i} 1i 8i 9g$	1
5	$f_{wwi} wxi xwi xxg$	$f_{0i} 2i 8i 10g$	1
6	$f_{wwi} wyi xwi xyg$	$f_{0i} 3i 8i 11g$	1
7	$f_{wwi} wzi ywi yzg$	$f_{0i} 1i 12i 13g$	1
8	$f_{wwi} wxi ywi yxg$	$f_{0i} 2i 12i 14g$	1
9	$f_{wwi} wyi ywi yyg$	$f_{0i} 3i 12i 15g$	1
10	$f_{wwi} zzi xxi yyg$	$f_{0i} 5i 10i 15g$	-1
11	$f_{wwi} zzi xxi yxg$	$f_{0i} 5i 11i 14g$	-1
12	$f_{wwi} zxj xzj yyg$	$f_{0i} 6i 9i 15g$	-1
13	$f_{wwi} zxj xyi yzg$	$f_{0i} 6i 11i 13g$	-1
14	$f_{wwi} zyi xzj yxg$	$f_{0i} 7i 9i 14g$	-1
15	$f_{wwi} zyi xxi yzg$	$f_{0i} 7i 10i 13g$	-1

Each of these 15 sets, or stabilizers, will yield 4 simultaneous eigenvectors, contributing 4 states to H_2 . We therefore recover the result that H_2 has 60 states. Subsets corresponding to entangled or product states can be distinguished by the product 'g' of the 3 corresponding Pauli matrices: a product equal to +1 corresponds to product states, while a product of -1 corresponds to entangled states. The number g can be thought as an entanglement 'index'.

We can obtain all the states of H_2 directly by forming a mixed linear combination of the first two non-identity elements from within each set. For instance $X_{3;12} = \frac{1}{2} (wy + i yw)$, when diagonalized, gives 4 orthogonal eigenvectors with four different eigenvalues⁵. We thus construct in the same manner 15 generalized X^0 's; each having a different principal axis, which we regard as the seed of H_2 : The result of the diagonalisation of the seed X^0 's gives the eigenvectors constituting H_2 : The following table lists the vectors corresponding to the eigenvalues (1 i). The vectors are not normalized for clarity. The vectors corresponding to stabilizers with $g = -1$ represent entangled states.

⁵Note that other rotations from s_2^1 ; such as

$X_{12;15} = \frac{1}{2} (12 + i 15)$

$X_{3;15} = \frac{1}{2} (3 + i 15)$;

will produce the same 4 eigenvectors, but with permuted eigenvalues.

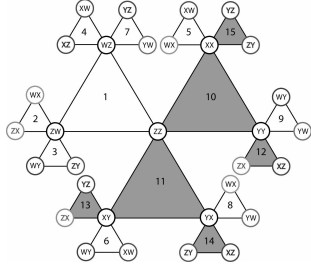


Figure 1:

1

Figure 1: Graph of the set formed by the 2-qubit generalized Pauli matrices P_j (circles bearing the subscript of the matrix in letter notation) and by the subsets of mutually-commuting matrices (triangles formed by 3 connected circles). The three '0's in a triangle share 4 common eigenvectors which form an orthonormal basis spanning the 2-qubit Hilbert space. The 15 triangles thus give 15 sets of 4 basis vectors. Shaded triangles correspond to entangled states ($g = -1$) while non-shaded triangles correspond to product states ($g = 1$). Neighbouring triangles have one (non-identity) vertex in common, and each (non-identity) vertex is shared by 3 triangles. The line segments adjoining the vertices of a triangle correspond to pairs f_j, g_k of commuting matrices and specifies a $\pi/2$ rotation $X_{j,k} = P_j + i P_k$ transforming the eigenvectors of an adjacent triangle into its neighbour.

Set	g	1 i	1 + i	1 i	1 + i
1	1	(0;0;0;1)	(0;1;0;0)	(0;0;1;0)	(1;0;0;0)
2	1	(0;0; 1;1)	(1;1;0;0)	(0;0;1;1)	(1;1;0;0)
3	1	(0;0;i;1)	(i;1;0;0)	(0;0; i;1)	(i;1;0;0)
4	1	(0; 1;0;1)	(0;1;0;1)	(1;0;1;0)	(1;0;1;0)
5	1	(1; 1; 1;1)	(1;1; 1;1)	(1; 1;1;1)	(1;1;1;1)
6	1	(i; 1;i;1)	(i;1;i;1)	(i; 1; i;1)	(i;1; i;1)
7	1	(0;i;0;1)	(0; i;0;1)	(i;0;1;0)	(i;0;1;0)
8	1	(i;i; 1;1)	(i; i; 1;1)	(i;i;1;1)	(i; i;1;1)
9	1	(1;i;i;1)	(1; i;i;1)	(1;i; i;1)	(1;i;i; 1)
10	1	(0; 1;1;0)	(1;0;0;1)	(1;0;0;1)	(0;1;1;0)
11	1	(i;0;0;1)	(0; i;1;0)	(0;i;1;0)	(i;0;0;1)
12	1	(1;1; 1;1)	(1;1;1;1)	(1; 1;1;1)	(1;1;1; 1)
13	1	(i; i;1;1)	(i; i; 1;1)	(i;i;1; 1)	(i;i;1;1)
14	1	(i;1; i;1)	(i;1;i;1)	(i; 1;i;1)	(i;1;i; 1)
15	1	(1; i;i;1)	(1;i; i;1)	(1; i; i;1)	(1;i;i;1)

Note that the first stabilizer of the product sector ($g = 1$) generates the computational basis, while the first stabilizer of the entangled sector ($g = -1$) generates the Bell basis.

This method not only finds the vectors of H_2 in an exhaustive way which does not make the computational basis play any special role (homogeneity). It also provides a road map for navigating between elements of H_2 . Consider three stabilizers which we call s_a , s_b and s_c . They have two generalized Pauli matrices in common, one of them being the trivial \mathbb{I} . We chose one of the two and call it s_m . Consider $3 \in \mathbb{F}_m$

$$\begin{aligned} j &\in s_a \\ k &\in s_b \\ l &\in s_c \end{aligned}$$

such that

$$f_{j; k} g = f_{k; l} g = f_{l; j} g = 0$$

Since all pairs of generalized Pauli matrices that do not commute must anti-commute, they also satisfy

$$[j; m] = [k; m] = [l; m] = 0$$

Then it is easy to show by a direct calculation that

$$X_m^a_j = \frac{1}{2} (i_m + i_j)$$

$$X_m^b_k = \frac{1}{2} (i_m + i_k)$$

$$X_m^c_l = \frac{1}{2} (i_m + i_l)$$

have one of the properties:

$$X_m^b_k X_m^a_j X_{k m}^b = X_m^c_l$$

or

$$X_m^b_k X_m^a_j X_{k m}^b = (X_m^c_l)^{-1} = -i X_{l m}^c$$

depending on whether the anti-commuting pair in the decomposition of i_k appear in cyclic order or anti-cyclic order, respectively. This means, following the proof given for the one-qubit case, that all the eigenvectors of s_a are transformed into the eigenvectors of s_c by the transformation X^b . It is easy to see that these last two relations can be straightforwardly generalized to N qubits.

All together, there are 120 different generalized $=2$ rotations generated by the scheme

$$X = \frac{1}{2} (i + i^0)$$

where i and i^0 commute.

An important remark is in order here. Among the X^0 's, a subset plays an important practical role. These are $=2$ rotations of the form

$$X_0^0_j = \frac{1}{2} (i_0 + i_j)$$

They correspond to the unitary time evolution

$$U(t) = e^{i^0_j t}$$

with $i^0 = -i$ and are thus directly implemented by an hamiltonian proportional to i_j :

They constitute the practical means of navigating in H_2 and more generally (see below) in H_N : They can be seen as the "primitives" of the Clifford group, as we will show.

We note that the generalized Pauli matrices in the above calculations are not limited to the two-qubit case, but can in fact be over N qubits. We therefore find that our generalized $=2$ rotations on N qubits, constructed from the subsets s_N^a , leave H_N invariant.

2.5 The generalized $=2$ rotations generate the C li ord group on N qubits

The N -qubit Pauli group G_N is defined as

$$G_N = f_w;_x;_y;_z g^N f_1;_i g$$

so that each element of the Pauli group is a tensor product of N Pauli matrices, up to an overall phase factor 1 ; i.e. The N -qubit C li ord group G_N is the normalizer of the Pauli group. That is, a unitary operator X is contained in C_N if and only if

$$X X^{-1} \in G_N \quad \forall X \in G_N$$

First, let us show that

$$X = \frac{j + i_k}{2} \in G_N \text{ if } [j;_k] = 0$$

We have

$$\begin{aligned} j_1 &= "j_1"_{1,j} \\ k_1 &= "k_1"_{1,k} \end{aligned}$$

where $"j_1" = 1$ and $"k_1" = 1$:

Thus,

$$\begin{aligned} X^{-1} X &= \frac{1}{2} (j + i_k)_{-1} (j - i_k) \\ &= \frac{1}{2}^{-1} ("j_1"_{-1,j} + i "k_1"_{-1,k}) (j - i_k) \\ &= \frac{1}{2} "j_1"_{-1} (j + i "k_1" "j_1"_{-1,k}) (j - i_k) \end{aligned}$$

If $"k_1" "j_1" = 1$;

$$\begin{aligned} &= \frac{1}{2} "j_1"_{-1} (2_0 + i_k j - i_j k) \\ &= "j_1"_{-1} \in G_N \end{aligned}$$

If $"k_1" "j_1" = -1$;

$$\begin{aligned} &= \frac{1}{2} "j_1"_{-1} (i_k j - i_j k) \\ &= i "j_1"_{-1} j_k \in G_N \end{aligned}$$

So the generalized $=2$ rotations on N qubits are elements of the C li ord group. Since the single qubit $=2$ rotations along with ICN OT form the minimal generators of the C li ord group [2], and ICN OT itself is just a product of two X 's (see below), our X 's also generate the C li ord group, which is the generalisation of the octahedral group to N -qubit.

2.6 Gates and generalized $\pi/2$ rotations on H_2

Any physical implementation of a qubit has a limited number of accessible gate operations. Determining the appropriate sequence of physical operations corresponding to some desired quantum gate is in general a difficult problem. Further, the language of quantum algorithms and quantum networks has been constructed by analogy from classical computing, and is not tailored to experimental protocols involving continuous rotations in Hilbert space. Our results provide a natural way to translate the language of quantum logic operations into that of geometry and help visualize what rotations should be performed. Consider, for instance, that the ISWAP gate,

$$\text{ISWAP} = \begin{matrix} & & & & 3 \\ & 1 & 0 & 0 & 0 \\ & 0 & 0 & i & 0 & 1 \\ & 0 & i & 0 & 0 & 5 \\ 2 & 0 & 0 & 0 & 1 & \\ & 0 & 0 & 0 & 1 & \end{matrix}$$

is given by

$$\begin{aligned} \text{ISWAP} &= \frac{1}{2} [w_w + z_z + i(x_x + y_y)] \\ &= \frac{1}{2} (w_w + i x_x) (w_w + i y_y) = X_{0;10} X_{0;15} \end{aligned}$$

The controlled phase shift rotation

$$\text{ICPHASE} = \begin{matrix} & & & & 3 \\ & 1 & 0 & 0 & 0 \\ & 0 & 1 & 0 & 0 & 1 \\ & 0 & 0 & i & 0 & 5 \\ 2 & 0 & 0 & 0 & 1 & \\ & 0 & 0 & 0 & i & \end{matrix}$$

is given by

$$\begin{aligned} \text{ICPHASE} &= \frac{1}{2} [w_w + z_w + i(w_z - z_z)] \\ &= \frac{1}{2} (w_w - i z_z) (w_w + i w_z) = i X_{5;0} X_{0;1} \end{aligned}$$

Finally the ICNOT,

$$\text{ICNOT} = \begin{matrix} & & & & 3 \\ & 1 & 0 & 0 & 0 \\ & 0 & 1 & 0 & 0 & 1 \\ & 0 & 0 & 0 & i & 5 \\ 2 & 0 & 0 & i & 0 & \\ & 0 & 0 & i & 0 & \end{matrix}$$

is given by

$$\begin{aligned}
\text{ICNOT} &= \frac{1}{2} [\text{ww} + \text{zw} + i(\text{wx} - \text{zx})] \\
&= \frac{1}{2} (\text{ww} - i\text{zx}) (\text{ww} + i\text{wx}) = iX_{6,0}X_{0,2}
\end{aligned}$$

This language makes it clear that each of these gates corresponds to two successive generalized $=2$ rotations having the same principal axis in H_2 :

A quantum computer whose evolution is limited to Clifford group gates and measurements (a Clifford quantum computer, so-to-speak) is not universal. The Gottesman-Knill theorem shows that such a quantum computer can be efficiently simulated on a classical computer [2]. Following in addition single-qubit $=4$ rotations (i.e. the $=8$ gate) leads to a universal set, but the cost is steep: we then lose the discretization of the space, and the relevant group leaving H_N invariant is now infinite. The Clifford group is nonetheless a very rich paradigm for quantum information processing. Quantum error-correcting codes, for example, use only Clifford group operations for encoding and decoding, while quantum cryptography and quantum teleportation can be performed with only Clifford group gates and measurements [1].

3 An alternative approach to discretization: shelling the high-dimensional dense lattices

The N -qubit Hilbert space is a high-dimensional space, and its multipartite nature (it is the tensor product of single-qubit Hilbert space) induces a subtle structure related to the state's various levels of entanglement [19], [20], which is not fully understood for $N \geq 3$. Instead of building the Hilbert space discretization from the above "algebraic" point of view, we will now address the same question from an a priori very different point of view, using high-dimensional dense lattices [15]. A very interesting fact is that both discretization schemes coincide for the one and two qubit cases, and maybe even for three qubits (see below).

Our strategy will be the following (we note $n = 2^N$). The normalization condition, together with writing complex numbers as pairs of real numbers, identifies the Hilbert space to the high-dimensional sphere S^{2n-1} embedded in \mathbb{R}^{2n} . In order to discretize these hyperspheres, we use the successive shells of dense lattices in \mathbb{R}^{2n} . At the same time, we must take into account the global phase freedom, and show how a discretization of the projective Hilbert space is induced. This means that several points on S^{2n-1} will represent the same physical state, as will be explained below. In the following, we call "qubit states" the quantum states associated to the points on S^{2n-1} , and "physical states" the states in the projective Hilbert space (which has the geometry of a complex projective space $\mathbb{C}P^{n-1}$). As in part 2, we here treat the cases for $N = 1$ and 2 .

The discretized one-qubit case is first presented in terms of the 24 vertices of a self dual polytope on S^3 , denoted $f3;4;3g$, which is the first shell of the densest packing in R^4 , denoted $_{_4}$. These 24 vertices corresponds to 24 one-qubit states, and, upon modding out the global phase, to 6 physical states. For the two-qubit case, we use the so-called Gosset polytope, the first shell of the densest packing in R^8 , denoted E_8 . We find that this polytope has 240 vertices leading to 240 two-qubit states, and further leading to 36 separable states and 24 maximally entangled physical states.

3.1 The one-qubit case

The generic state reads

$$j_i = t_0 j_0 i + t_1 j_1 i; \text{ and } j_0^2 + j_1^2 = 1$$

The normalization condition identifies the set of normalized states to the S^3 sphere embedded in R^4 : The projective case (the set of states modulo a global phase) leads to the Bloch sphere description, which can be seen as the base of the S^3 Hopf fibration [6] [7]. An interesting discrete model on S^3 is provided by the self dual $f3;4;3g$ polytope [17]. It is related to the "Hurwitz" quaternion group. We now give two possible (dual) coordinates for its vertices, in each case as a real quadruplet and a complex pair. The correspondance between real quadruplets and complex pairs amounts simply to taking the first two (last two) real numbers as the real and imaginary part of the first (second) complex number. The first (the second) complex number in the pair corresponds to t_0 (t_1).

A first set, denoted T_1 , is the union of the 8 permutations of type $(1;0;0;0)$ and the 16 permutations of type $\frac{1}{2}(1;1;1;1)$. Note that, modulo a global phase factor, these 24 points really represent 6 different physical states, which appear on the Bloch sphere as opposite points on the three orthogonal axes $x; y; z$. Indeed, the four points

real quadruplets	complex pairs
$(1;0;0;0)$	$(1;0)$
$(-1;0;0;0)$	$(-1;0)$
$(0;1;0;0)$	$(i;0)$
$(0; -1;0;0)$	$(-i;0)$

represent the states $j_1; i = e^{i\pi} j_0 i$, with $i = 0; 1; 2; 3 = 2$, which map to the same point on the Bloch sphere (the north pole). They are therefore associated to the physical state $j_1 i$. Equivalently, the four points

real quadruplets	complex pairs
$(0;0;1;0)$	$(0;1)$
$(0;0; -1;0)$	$(0; -1)$
$(0;0;0;1)$	$(0;i)$
$(0;0;0; -1)$	$(0; -i)$

represent the 4 states $j_2; i = e^{i\pi} j_1 i$ with $i = 0; =2; ;3 =2$. The 16 other vertices represent 4 other physical states, in the following way:

$$\begin{aligned}
 j_{3i} & \xrightarrow{e^{i(\pi/2)} = 4} (j_1 i \quad j_1 i) \\
 j_{4i} & \xrightarrow{e^{i(\pi/2)} = 4} (j_1 i \quad j_1 i) \\
 j_{5i} & \xrightarrow{e^{i(\pi/2)} = 4} (j_1 i + i j_1 i) \\
 j_{6i} & \xrightarrow{e^{i(\pi/2)} = 4} (j_1 i \quad i j_1 i)
 \end{aligned}$$

with $i = 0; =2; ;3 =2$

For the later purpose of a discrete two-qubit construction (see below), it is useful to describe a second version of the polytope $f3;4;3g_p$ for which the 24 vertices form a set T_2 , made of 24 permutations of the type $1 = 2 f 1; 1; 0; 0 g$: This polytope is just obtained from the former one through a screw motion on S^3 of angle $\pi/4$: This set leads to 24 states

$$j_{1i}; i = j_{1i}; i; i = 1; 6; i = 0; =2; ;3 =2, \text{ and } = e^{i\pi/4}$$

and to the six one-qubit physical states j_{1i} identical to j_{1i} : Indeed, the six states j_{1i} sit at the vertices of a regular octahedron. Since the states j_{1i} only differ from j_{1i} by a global phase, they map onto the same six points on the Bloch sphere.

3.2 The two-qubit case

We now consider the case of two qubits, which reads:

$$j_i = t_{00} j_0 i + t_{01} j_0 1 i + t_{10} j_1 0 i + t_{11} j_1 1 i; \text{ and } j_{00}^2 + j_{01}^2 + j_{10}^2 + j_{11}^2 = 1$$

The normalisation condition identifies the set of normalised states to the sphere S^7 : As for the one qubit case, we choose to consider the first shell of points in the densest lattice in R^8 , denoted E_8 :

This lattice belongs to the family of lattices E_8 , and is therefore sometimes denoted E_8 . These lattices form a series which starts with the triangular lattice in 2d (the densest lattice in 2d). E_3 is obtained as a particular sequence of E_2 lattices packed in a third dimension, which gives the face centered cubic lattice, one of the two densest lattices in 3d. Packing adequately E_3 lattices along a fourth dimension leads to E_4 , whose first shell is precisely the above used $f3;4;3g_p$ polytope. Upon iteration, this construction eventually leads to the $E_8 = E_8$ lattice suitable for the two-qubit case. For the present purpose, we shall mainly focus on the set of 240 sites belonging to the E_8 first shell, which form the so-called Gosset polytope, and along the same line as for the one qubit case, enumerate the physical states they represent.

3.3 Discrete Hopf bration for the Gosset polytope on S^7

The 240 vertices of the Gosset polytope belong to an S^7 sphere. It is interesting to split these 240 vertices into 10 equivalent subsets, each belonging to non-intersecting S^3 spheres. This is nothing but a discrete version of the S^7 Hopf bration, with fibers S^3 and base S^4 [18], [8], [7], [19].

It is simpler to use here quaternionic coordinates instead of complex or real ones. The above set T_1 , scaled such that the corresponding points belong to a sphere S^3 of radius $\frac{1}{2}$ reads now :

$$T_1 = f \left(\frac{1}{2} \mathbf{i}, \frac{1}{2} \mathbf{j}, \frac{1}{2} \mathbf{k} \right) \left(1 \quad \mathbf{i} \quad \mathbf{j} \quad \mathbf{k} \right) g;$$

where \mathbf{i}, \mathbf{j} and \mathbf{k} are the standard unit quaternions. The set T_2 stays on a unit sphere and reads:

$$T_2 = f \left(\frac{1}{2} \mathbf{i}, \frac{1}{2} \mathbf{j}, \frac{1}{2} \mathbf{k} \right) \left(1 \quad \mathbf{j} \right) \left(1 \quad \mathbf{k} \right) \left(\mathbf{i} \quad \mathbf{j} \right) \left(\mathbf{i} \quad \mathbf{k} \right) \left(\mathbf{j} \quad \mathbf{k} \right) g$$

The 240 Gosset polytope vertices belong to the 10 sets:

$$\begin{aligned} S_1 &= (T_2; 0); \quad S_2 = (0; T_2); \quad S_{3,4} = (T_1; \quad T_1); \quad S_{5,6} = (T_1; \quad i T_1); \\ S_{7,8} &= (T_1; \quad j T_1); \quad S_{9,10} = (T_1; \quad k T_1) \end{aligned}$$

This notation means the following. For the numbers which appear as indices in S , the first (resp. the second) refers to the sign plus (resp. minus) in the second term of the pair. One therefore considers pairs $(q_1; q_2)$ of identical quaternions in T_1 , the second being multiplied on the left by the specified unit (with the correct sign) to give the pair $(q_1; q_2)$, and finally a corresponding point in \mathbb{R}^8 .

Each of the ten sets gives a copy of a $f3;4;3g$ polytope on a fibre S^3 . The points can be Hopf mapped, as described elsewhere [19] onto the base space S^4 . The location of the mapped point is intimately related to the entanglement content of the corresponding two-qubit state. Indeed, the Hopf map is simply described as a first map which sends the pair $(q_1; q_2)$ onto the quaternion $Q = \underline{q_1 q_2}^{-1}$ (which is sent to infinity if $q = 0$), followed by an inverse stereographic map which sends Q to S^4 : A main result is that the Hopf map is sensitive to entanglement: for separable states, Q is simply a complex number, not a generic quaternion; on the contrary, for maximally entangled states (MES), the purely complex part of Q vanishes. This translates onto the base S^4 in the following way. Embed S^4 into \mathbb{R}^5 ; with coordinates $fx_1; l = 0 \quad 4g$: Separable states are such that $x_3 = x_4 = 0$, and the S^2 sphere spanned by $fx_0; x_1; x_2 g$ form the standard Bloch sphere of the first qubit. Maximally entangled states map onto the unit circle in the plane $(x_3; x_4)$. Note that a well-known entanglement measure, the concurrence [11], is simply given by the radius in the plane $(x_3; x_4)$: $C = \sqrt{x_3^2 + x_4^2}$, an expression which will be used later.

In the present case, it is then easy to verify that the sets S_1 to S_6 correspond to separable states, while sets S_7 to S_{10} correspond to maximally entangled (Bell

like) states. The correspondance between vertices and states is done by transforming back the quaternion pairs into complex quadruplets whose terms are $(t_{00}; t_{01}; t_{10}; t_{11})$. More precisely, the $(q_1; q_2)$ pair reads $(t_{00} + t_{01}j; t_{10} + t_{11}j)$: Note that the quaternion unit j acts on the right of the complex numbers, while it acts on the left in the definition of $S_{1,8}$. Since quaternion multiplication is non-commutative, this distinction is important in going back and forth between the lattice points and the states.

3.4 The separable states

As an example, consider the set S_1 , corresponding to the 24 states such that $t_{10} = t_{11} = 0$, and which reads

$$j i_1 \quad j i_2; i_1; i_2 = 0; =2; =3 =2; \text{ and } l = 1::6$$

As a whole, the six sets $S_1 \dots S_6$ encompass 6 \times 24 = 144 sites, forming altogether 36 physical states, with four values of the global phase for each such state. Note that the precise value of the phases are important here in such a way that our discretization procedure covers as regularly as possible the full Hilbert space. Using the above defined eigenstates of the one-qubit Pauli matrices, these states read

$$\begin{aligned} & j x i \quad j x i e^{i(\pi/4 + m\pi/2)} \\ & j y i \quad j y i e^{i(\pi/4 + m\pi/2)} \\ & j z i \quad j z i e^{i(\pi/4 + m\pi/2)} \\ & j x i \quad j y i e^{i(\pi/4 + m\pi/2)} \\ & j y i \quad j x i e^{i(\pi/4 + m\pi/2)} \\ & j x i \quad j z i e^{im\pi/2} \\ & j z i \quad j x i e^{im\pi/2} \\ & j y i \quad j z i e^{im\pi/2} \\ & j z i \quad j y i e^{im\pi/2} \end{aligned}$$

where $m = 0; 1; 2; 3$ triggers the global phase and each of the 9 lines stands for the 4 combinations of signs \pm , leading to the announced 36 physical states. A simple view of these separable states consists in relating them to the "product" of two octahedra, each one belonging to the Bloch sphere of the individual qubits

3.5 The maximally entangled states

The remaining four sets (altogether 4 \times 24 = 96 sites) leads to a slightly more subtle structure. One finds as a whole 24 different physical states, with 4 phase-distinct two-qubit states for each. But in the present case, these 4 latter states belong to two different sets, either $(S_7; S_8)$ or $(S_9; S_{10})$

As an example, let us consider the set S_7 and enumerate the states equivalent to, say, the quaternion pair $\left(\frac{1}{2}; \frac{1}{2}\right)$ $\in T_1$, which translates into the complex quadruplet $(\frac{1}{2}; 0; 0; \frac{1}{2})$ and therefore to the MES:

$$M \in S_1; 0i = \frac{1}{2} (j0i + j1i) = \frac{1}{2} (jz; + zi + jz; - zi)$$

The shortened notation $jz; + zi$ stands for $jz_1 - jz_2$: There is only one other element in S_7 ; the pair $\left(\frac{1}{2}; -\frac{1}{2}\right)$, corresponding to $M \in S_1; i = e^i M \in S_1; 0i$: The other two elements belong to the set S_8 and read $\left(\frac{1}{2}; \frac{k}{2}\right)$ and $\left(\frac{j}{2}; \frac{k}{2}\right)$; associated respectively to the states $M \in S_1; =2i$ and $M \in S_1; =-2i$. Before giving the full list of states, it is interesting to focus on the next 3 states in S_7 , generated by $i; j$ and k , respectively. One gets respectively

$$\begin{aligned} M \in S_2; 0i &= \frac{i}{2} (j0i - j1i) = \frac{i}{2} (jz; + zi - jz; - zi) \\ M \in S_3; 0i &= \frac{1}{2} (j1i + j0i) = \frac{1}{2} (jz; - zi + jz; - zi) \\ M \in S_4; 0i &= \frac{i}{2} (j1i - j0i) = \frac{i}{2} (jz; - zi - jz; - zi) \end{aligned}$$

The set $\{M \in S_1; 0i, M \in S_2; 0i, M \in S_3; 0i, M \in S_4; 0i\}$ forms precisely the entangled "magic" basis described elsewhere. [9], [10] Each physical state $M \in S_1$ corresponds to the 4 two-qubit states $M \in S_1; !i$, with $! = 0$ for states in S_7 and $! = 1, 2, 3$ for states in S_8 : As a whole, the 48 vertices of the sets S_7 and S_8 provide 12 physical MES, each one representing a set of four phase-related states. They are listed below, in the $! = 0$ case, and with $= e^{i\pi/4}$:

$$\begin{aligned} M \in S_5; 0i &= \frac{-}{2} (j0i + j1i) - \frac{-}{2} (j1i - j0i) = \frac{p}{2} (jz; + xi + ijz; - xi) \\ M \in S_6; 0i &= \frac{-}{2} (j0i - j1i) + \frac{-}{2} (j1i + j0i) = \frac{p}{2} (jz; - yi + jz; - yi) \\ M \in S_7; 0i &= \frac{-}{2} (j0i - j1i) + \frac{-}{2} (j1i + j0i) = \frac{p}{2} (jz; + yi - jz; - yi) \\ M \in S_8; 0i &= \frac{-}{2} (j0i + j1i) - \frac{-}{2} (j1i - j0i) = \frac{p}{2} (jz; + xi - ijz; - xi) \\ M \in S_9; 0i &= \frac{-}{2} (j0i - j1i) + \frac{-}{2} (j1i + j0i) = \frac{p}{2} (jz; - xi - ijz; - xi) \\ M \in S_{10}; 0i &= \frac{-}{2} (j0i + j1i) - \frac{-}{2} (j1i - j0i) = \frac{p}{2} (jz; + yi + jz; - yi) \\ M \in S_{11}; 0i &= \frac{-}{2} (j0i + j1i) - \frac{-}{2} (j1i - j0i) = \frac{p}{2} (jz; - yi + jz; - yi) \\ M \in S_{12}; 0i &= \frac{-}{2} (j0i - j1i) + \frac{-}{2} (j1i + j0i) = \frac{p}{2} (jz; - xi + ijz; - xi) \end{aligned}$$

The latter 12 physical states are read out from the two sets S_9 and S_{10} :

$$\begin{aligned}
 \mathcal{M} E S_{13};0i &= \frac{1}{2} \mathcal{P}_{0i} + \frac{i}{2} \mathcal{P}_{1i} = \frac{1}{2} (\mathcal{P}_{z+} z; + \mathcal{P}_{z-} z; - \mathcal{P}_{z+} z; - \mathcal{P}_{z-} z;) \\
 \mathcal{M} E S_{14};0i &= \frac{i}{2} \mathcal{P}_{0i} + \frac{1}{2} \mathcal{P}_{1i} = \frac{1}{2} (\mathcal{P}_{z+} z; + \mathcal{P}_{z-} z; - \mathcal{P}_{z+} z; - \mathcal{P}_{z-} z;) \\
 \mathcal{M} E S_{15};0i &= \frac{1}{2} \mathcal{P}_{0i} + \frac{i}{2} \mathcal{P}_{1i} = \frac{1}{2} (\mathcal{P}_{z+} z; - \mathcal{P}_{z-} z; + \mathcal{P}_{z+} z; - \mathcal{P}_{z-} z;) \\
 \mathcal{M} E S_{16};0i &= \frac{i}{2} \mathcal{P}_{0i} + \frac{1}{2} \mathcal{P}_{1i} = \frac{1}{2} (\mathcal{P}_{z+} z; - \mathcal{P}_{z-} z; - \mathcal{P}_{z+} z; + \mathcal{P}_{z-} z;) \\
 \mathcal{M} E S_{17};0i &= \frac{1}{2} (\mathcal{P}_{0i} + \mathcal{P}_{1i}) - \frac{1}{2} (\mathcal{P}_{0i} - \mathcal{P}_{1i}) = \frac{1}{2} (\mathcal{P}_{z+} z; + \mathcal{P}_{z-} z; - \mathcal{P}_{z+} z; - \mathcal{P}_{z-} z;) \\
 \mathcal{M} E S_{18};0i &= \frac{1}{2} (\mathcal{P}_{0i} - i \mathcal{P}_{1i}) + \frac{1}{2} (i \mathcal{P}_{0i} + \mathcal{P}_{1i}) = \frac{1}{2} (\mathcal{P}_{z+} z; - \mathcal{P}_{z-} z; + \mathcal{P}_{y+} y; - \mathcal{P}_{y-} y;) \\
 \mathcal{M} E S_{19};0i &= \frac{1}{2} (\mathcal{P}_{0i} - i \mathcal{P}_{1i}) - \frac{1}{2} (i \mathcal{P}_{0i} + \mathcal{P}_{1i}) = \frac{1}{2} (\mathcal{P}_{z+} z; - \mathcal{P}_{z-} z; - \mathcal{P}_{y+} y; - \mathcal{P}_{y-} y;) \\
 \mathcal{M} E S_{20};0i &= \frac{1}{2} (\mathcal{P}_{0i} + \mathcal{P}_{1i}) - \frac{i}{2} (\mathcal{P}_{0i} - \mathcal{P}_{1i}) = \frac{1}{2} (\mathcal{P}_{z+} z; + \mathcal{P}_{z-} z; - \mathcal{P}_{x+} x; - \mathcal{P}_{x-} x;) \\
 \mathcal{M} E S_{21};0i &= \frac{1}{2} (\mathcal{P}_{0i} - \mathcal{P}_{1i}) + \frac{i}{2} (\mathcal{P}_{0i} + \mathcal{P}_{1i}) = \frac{1}{2} (\mathcal{P}_{z+} z; - \mathcal{P}_{z-} z; + \mathcal{P}_{x+} x; - \mathcal{P}_{x-} x;) \\
 \mathcal{M} E S_{22};0i &= \frac{1}{2} (\mathcal{P}_{0i} + i \mathcal{P}_{1i}) - \frac{1}{2} (i \mathcal{P}_{0i} + \mathcal{P}_{1i}) = \frac{1}{2} (\mathcal{P}_{z+} z; + \mathcal{P}_{z-} z; - \mathcal{P}_{y+} y; - \mathcal{P}_{y-} y;) \\
 \mathcal{M} E S_{23};0i &= \frac{1}{2} (\mathcal{P}_{0i} + i \mathcal{P}_{1i}) - \frac{1}{2} (i \mathcal{P}_{0i} - \mathcal{P}_{1i}) = \frac{1}{2} (\mathcal{P}_{z+} z; - \mathcal{P}_{z-} z; + \mathcal{P}_{y+} y; - \mathcal{P}_{y-} y;) \\
 \mathcal{M} E S_{24};0i &= \frac{1}{2} (\mathcal{P}_{0i} - \mathcal{P}_{1i}) + \frac{i}{2} (\mathcal{P}_{0i} + \mathcal{P}_{1i}) = \frac{1}{2} (\mathcal{P}_{z+} z; - \mathcal{P}_{z-} z; - \mathcal{P}_{x+} x; - \mathcal{P}_{x-} x;)
 \end{aligned}$$

As a whole, the 96 M E S two-qubits states read

$$\mathcal{M} E S_1; i = e^{i!} \mathcal{M} E S_1; 0i; \text{with } ! = 0; = 2; ; 3 = 2 \text{ and } l = 1 \quad 24$$

Adding out the global phase, we can write the 24 physical states in the

form

$$\begin{aligned}
 \frac{1}{2} & \quad j \cdot z; + z_i + e^i \ j \ z; \ z_i \\
 \frac{1}{2} & \quad j \cdot z; \ z_i + e^i \ j \ z; z_i \\
 \frac{1}{2} & \quad j \cdot z; + x_i + e^i \ j \ z; \ x_i \\
 \frac{1}{2} & \quad j \cdot z; \ x_i + e^i \ j \ z; + x_i \\
 \frac{1}{2} & \quad j \cdot z; + y_i + e^i \ j \ z; \ y_i \\
 \frac{1}{2} & \quad j \cdot z; \ y_i + e^i \ j \ z; + y_i
 \end{aligned}$$

with $= 0; = 2; ; 3 = 2$

Note that these 24 maximally entangled states, together with the above 36 separable states, are equivalent, up to a global phase, to the 60 states derived in the first part of this paper.

3.6 New states on the next E_8 shells

The E_8 first shell has therefore provided a nice discretization of the two-qubit Hilbert space, in the sense that it already contains separable and maximally entangled states. As a comparison, the first shell of the hypercubic lattice in 8 dimensions (with its 16 vertices) would only lead to separable states. The high symmetry of this set of 240 two-qubit states is read out from the point group symmetry of E_8 , and therefore of the 240 vertex Gosset polytope, which has a huge order [16]: $696\,729\,600 = 2^{14} \cdot 3^5 \cdot 5^2 \cdot 7$.

A next step consists in considering the higher order shells in E_8 , which will provide symmetrical two-qubit states of intermediate entanglement. A word of caution should be made here, since we are only interested in describing normalized quantum states. Lattice points which are aligned, as viewed from the origin, contribute to the same two-qubit state. One should therefore only focus on the so-called lattice "visible points", which form the Möbius transform of the lattice [14].

We will not give here a detailed description of the new two-qubit states that are associated with these higher shells. But a nice property of E_8 shelling allows one to simply enumerate the new level of entanglement carried by these shells. Let us first note that the number M_J of sites on the J^{th} shell around an E_8 vertex is simply given by [15]

$$M_J = 240 \sum_{d|J} \frac{X}{d^3}$$

where d denotes integers which divide J . The table below displays these numbers for the first four shells.

J	1	2	3	4
M	240	2160	6720	17520

The shell by shell analysis, and its relation to the Hopf map was done elsewhere [8], [7]. It allows us to get points on the second shell corresponding to states having concurrence $0; 1=2; 1=\frac{1}{2}; 1$. The third shell contributes states of concurrence $0; 1=3; 2=3; \frac{1}{2}=3; \frac{1}{2}=3; 1=3$ and 1:

3.7 Discrete one-qubit mixed states

It is well known that the full set of one-qubit mixed states can be obtained by tracing out one qubit of generic two-qubit pure states. Mixed states are represented by points inside the so-called "Bloch ball", bounded by the pure state Bloch sphere. In the context of generalizing the Bloch sphere for two-qubit pure states using the S^7 Hopf fibration [9], it was shown that the Bloch ball corresponds precisely to the restriction to the triplet $(x_0; x_1; x_2)$ on the base space S^4 . This describes mixed states obtained upon tracing out the second qubit. It is then tempting to propose, in parallel to the two-qubit pure state discretization, an E_8 -related discretisation of the Bloch ball.

From the E_8 first shell, one gets the 6 permutations $(1; 0; 0)$, corresponding to pure states on the Bloch sphere (the traced separable two-qubit states) forming an octahedron. One also gets the point $(0; 0; 0)$, the Bloch ball centre, corresponding to traced maximally entangled states.

From the E_8 second shell, we find in addition the 8 permutations $\frac{1}{2}; \frac{1}{2}; \frac{1}{2}$; a cube of radius $\frac{\sqrt{3}}{2}=2$ and the 12 permutations $\frac{1}{2}; \frac{1}{2}; 0$; a cuboctahedron of radius $1=\frac{\sqrt{2}}{2}$. The Bloch ball can be further discretized by using traced states originating from E_8 higher shells.

3.8 Perspectives

As for the one- and two-qubit cases, the three-qubit Hilbert space geometry can be addressed in terms of high-dimensional sphere Hopf fibrations. Although the full entanglement properties are not described as nicely as in the two-qubit case, the S^{15} Hopf map is still found to be entanglement sensitive [12], [13]. Along the present dense lattice strategy, the three-qubit case should be related to the dense lattice \mathbb{Z}^{16} in \mathbb{R}^{16} (a case which is presently under study). The number of lattice sites closest to the origin (the so-called "lattice kissing number") is 4320 for the \mathbb{Z}^{16} , which is precisely four times the expected number of vertices on the uniform Hilbertian polytope H_3 (see section 2). We therefore face a similar situation as in the one- and two-qubit cases, where the factor of four accounted for the fourphase-related qubit states for each physical state. However, the four-to-one relation between the \mathbb{Z}^{16} first shell sites and the vertices of H_3 remains to be checked. It will clearly be very interesting to analyze the extent to which, for larger N , the stabilizer and dense lattice approaches to discretization still coincide.

Acknowledgment 2 Two of us, M.D. and C.R., are indebted to Ike Chuang for his enthusiastic teaching of quantum information theory and to Daniel Gottesman for communicating and explaining his results. In addition, R.M. would like to thank Perola Milmari and Karol Zyczkowski for interesting discussions and comments on the 2 qubits Hilbert space geometry. Daniel E. Steve and Dennis V. Vion are also gratefully acknowledged by all of us for helpful interactions. Finally, John Preskill's web-accessible notes and exercises on quantum information have been very useful.

References

- [1] D. Gottesman, arXiv e-print quant-ph/9807006.
- [2] D. Gottesman, *Stabilizer Codes and Quantum Error Correction*. Ph.D. thesis, California Institute of Technology, Pasadena, CA, 1997. arXiv e-print quant-ph/9705052.
- [3] M. A. Nielsen and I.L. Chuang, *Quantum Computation and Quantum Information* (Cambridge University Press, Cambridge, 2000), Chap. 10.
- [4] D. Gottesman, personal communication
- [5] J. Dehaene and B. De Moor, Phys. Rev. A 68, 042318 (2003).
- [6] H. Uebelake, American Journal of Physics, 59 (1991) page 53
- [7] J.F. Sadoc and R. Mosseri, *Geometric Frustration*, Cambridge University Press 1999)
- [8] J.F. Sadoc and R. Mosseri, J. Phys. A : Math. Gen. 26 (1993) 1789-189
- [9] C.H. Bennett, D.P. DiVincenzo, J. Smolin and W.K. Wootters, Physical Review A, 54, 3824 (1996)
- [10] S. Hill and W.K. Wootters, Phys. Rev. Lett. 78 (1997) 5022
- [11] W.K. Wootters, Phys. Rev. Lett. 80 (1998) 2245
- [12] R. Mosseri, quant-ph/0310053
- [13] B.A. Bernevig and H.D. Chen, J. Phys. A : Math. Gen., 36 (2003) 8325
- [14] R. Mosseri, J. Phys. A : Math. Gen. 25 (1992) L25-L29.
- [15] Conway and Sloane 1988 'Sphere packings, lattices and groups' (Springer Verlag)
- [16] V. E. Ller and N.J.A. Sloane, J. Phys. A : Math. Gen. 20 (1987) 6161-6168
- [17] Coxeter H. S. M. 1973 'Regular Polytopes' (Dover)

- [18] M anton N S , Comm .M ath. Phys.113 (1987) 341-351
- [19] M osseri R . and D andolo R , J.of Phys.A :M ath. G en. 34 (2001) 10243-10252
- [20] M .K us and K .Zyczkowski, Phys.Rev.A 63 (2001) 032307